Flow dependent predictability of the North Atlantic jet

T. H. A. Frame[1,2] , J. Methven[2], S. L. Gray[2] and M. H. P. Ambaum[2]

November 11, 2012

Abstract

The North-Atlantic eddy-driven jet is a major component of the large-scale flow in the northern-hemisphere. Here we present evidence from reanalysis and ensemble forecast data for systematic flow-dependent predictability of the jet. It is found that when the jet is weakened or split it is both less persistent and less predictable. This suggests that as the jet weakens or splits it enters into a state more sensitive to small differences between ensemble forecast members, rather like the sensitive region between the wings of the Lorenz attractor. When the jet is shifted poleward of its mean latitude it is more likely to weaken and transition to an equatorward shifted state via wave-breaking, hence passing through this sensitive state. This may provide an explanation for lower probabilistic forecast skill as the jet is initial in a poleward shifted state.

[1]NCAS Weather
[2]Department of Meteorology, University of Reading.

Correspondence address:
Department of Meteorology, University of Reading, Earley Gate, Reading, RG6 6BB, United Kingdom.
Email: t.h.a.frame@reading.ac.uk

1 Introduction

Mid-latitude atmospheric jets are of great importance to the climate and weather forecasting alike. In particular anomalous weather patterns over Europe have often been associated with excursions of the North Atlantic jet. The North-Atlantic jet is often partitioned into a vertically confined upper-level jet-stream and a barotropic, eddy-driven component. Recent results (*Woollings et al.*, 2010; *Franzke et al.*, 2012; *Hannachi et al.*, 2012) have suggested that climate statistics of the North-Atlantic eddy driven jet possess significant inhomogeneities indicating the presence of three regimes: a regime with the maximum wind-speed of the jet shifted south of its climatological mean latitude, one with it close to the mean latitude and one with it shifted north of the mean latitude. Further evidence has been found that the skill in forecasting the jet appears to vary with these regimes, with the skill being lowest when the forecast starts with the jet in the north regime (*Frame et al.*, 2011). These differences in forecast skill could indicate the presence of flow dependent predictability; i.e. the predictability of the jet depends systematically on its current state.

In this paper the evidence for flow dependent predictability of the North Atlantic eddy-driven jet during northern-hemisphere winter (DJF) is examined. The main aims are to identify properties from climatological data which link the frequency distribution of the jet to its evolutionary behavior, and to determine whether the predictability of the jet shows flow dependence consistent with these properties.

The rest of the paper is divided into four sections. In section 2, a two-dimensional principal component space in which we will explore the properties of the jet is described. In section 3 the frequency distribution and evolutionary behavior within this two-component principal component space is examined, using climatological data taken from the European Centre for Medium Range Weather Forecasts (ECMWF) reanalysis data-set (ERA-40) (*Uppala et al.*, 2005). In section 4 the predictability of the jet is examined, using ECMWF ensemble forecast data taken from the THORPEX Interactive Grand Global Ensemble (TIGGE) data-set (*Park et al.*, 2008). Finally a summary of the main results and conclusions of the paper is presented in section 5.

2 Characterization of the Eddy driven jet using principal components

In the work presented in this paper, a two-dimensional coordinate system will be used to describe the variability of the North-Atlantic eddy-driven jet. In this coordinate system the coordinate axes are scaled such that they are proportional to the square-root of kinetic energy, and the amplitude and latitude of the maximum wind-speed are approximate radial and angular coordinates respectively. This particular set of coordinates is chosen as it encapsulates the jet diagnostics of *Woollings et al.* (2010) whilst using a physically normalized coordinate system which is directly related to the variables of dynamical equations. The coordinate system is derived using principal component analysis (*Jolliffe*, 2002) applied to ERA-40 zonal wind data. The principal component calculations, and the properties of the resultant principal component space (hereafter PC-space) are summarized below.

As in *Woollings et al.* (2010) and *Frame et al.* (2011) the North-Atlantic eddy-driven jet is defined from the zonal winds between 15°N and 75°N zonally averaged between 60°W and 0°W and vertically averaged between the 925hPa and 750hPa pressure levels. This method of averaging produces profiles of zonal wind as a function of latitude. Such profiles are calculated for each 6 hourly time-point in the ERA-40 data-set. The time mean profile is then subtracted and the profiles weighted by the square-root of cosine of latitude. Since the data is on a regular latitude-longitude grid, this weighting means that the inner-product is proportional to kinetic energy. The data is then decomposed into principal components (PCs) and associated Empirical Orthogonal Functions (EOFs). This decomposition transforms the data into an orthogonal set of spatial structures (EOFs) whose amplitude coefficients (PCs) are uncorrelated in time. The PC-EOF pairs are sorted in descending order such that the first pair accounts for the largest fraction of the total variance and the last the smallest fraction.

The basic properties of the principle component decomposition are summarized in Figure 1. Figure 1a shows the percentage of the total variance explained by the leading 34 PC-EOF pairs. The stepped structure of Figure 1a indicates that the leading PC-EOF pairs should be grouped into twos, each group accounting for roughly equal variance. The first group of two PC-EOF pairs account for more than 40% of the variance.

The zonal wind profiles associated with the first group of two EOFs (EOF1 and EOF2) are plotted in Figure 1b, along with the time mean zonal wind profile. The plotted EOFs have been scaled to have amplitude of one standard deviation. The EOFs in this first group are similar in structure to those found for simulated data by *Monahan and Fyfe* (2006, 2009), and may be considered "typical" zonal jet EOFs. In combination with the mean they are sufficient to describe the large-scale variability of jet; allowing for northward and southward shifts as well as amplification of the jet. The EOFs in the second (3 and 4) third group (5 and 6) have similar wave-like structure but are of double and triple wavenumber respectively.

Figure 1c shows the relationship between the amplitudes (PCs) of the first two EOFs and the latitude and amplitude of the jet maximum. The coordinate axes are normalized by the pooled standard deviation of the first two PCs and are proportional to the square-root of kinetic energy. The white contours show the total square-root-kinetic energy contained in the first two PCs, including the contribution from the time-mean. The red/filled contours and black contours show the magnitude (ms^{-1}) and latitude of the jet maximum respectively. As in the *Woollings et al.* (2010) the jet maximum is defined as the maximum zonal wind speed, and the jet latitude as the latitude location at which the jet maximum occurs. The stippling in Figure 1c indicates a region of PC-space in which two distinct jet maxima occur, when this occurs the jet is defined as the maxima with the largest magnitude. The thick black contour between 35°N and 60°N in Figure 1c demarks the point at which the two separate maxima have equal magnitude. Crossing this boundary in a clockwise direction implies the decay of the jet in the north with a growth of the jet in the south; the converse being true for anti-clockwise crossing.

3 Frequency and Persistence of the jet

We have so far described a two dimensional principal component space (PC-space) in which the latitude and amplitude of the eddy-driven jet appear as approximate angular and radial coordinates respectively, and the inner-product is proportional to kinetic energy. We shall now consider the frequency distribution of points in that space and how this relates to the way in which trajectories move through the space. In particular we shall show that the frequency distribution is distorted from a pure Gaussian shape, and that these distortions appear to be associated with differences between the residence time (i.e. persistence) of trajectories in different regions of the PC-space. Furthermore we shall show that variations in the typical

distance traveled along trajectories in two days is a reasonably robust indicator of these variations in residence time.

To examine the behavior of trajectories we shall use 45-winters of six-hourly ERA-40 data sampled every two days, providing a total of 2025 data points. The two-day sampling frequency is chosen because two days was found to be the shortest time-scale for which a linear constant coefficient first order auto-regressive model (hereafter AR1 model) fit the auto-correlation function of the data. The two-day time-scale was identified and AR1 model fitted using software and methods described by *Schneider and Neumaier* (2001) and *Neumaier and Schneider* (2001). The AR1 model is sufficient to explain the mean, variance, auto-correlation and distribution of increment lengths of the data, it therefore provides a useful null hypothesis for testing whether local variations in behavior require "interesting" (*Christiansen*, 2009) explanations, beyond a random walk (*Stephenson et al.*, 2000).

It is important to note that with a two-day sampling frequency the notion of local (in PC-space) evolution still makes sense. For example 68% of two-day increments have magnitude less than one PC-unit, 95% less than 1.65 PC-units and maximum distance traveled in two days is ∼2.7 PC-units. Over 99% of data-points from the full six-hourly data set lie within a distance 0.7 PC-units of a line joining the end-points of a two-day increment and the maximum distance any point lies from the line is 1.07 PC-units. Therefore, sub-sampling the data does not averaging out large excursions and mask significantly non-local behavior.

The first thing we shall consider is the distribution of the data-points in PC-space. A kernel smoothing estimate of the frequency distribution is shown in Figure 2a. As in Figure 1c the black contours and white contours show the jet latitude and the square-root of energy. A flat circular kernel of radius 0.78 PC-units was used to produce this estimate. This radius is the median length of two day PC-space increments. The black circle in the top right illustrates the size of the kernel. Since the kernel is flat, the frequency distribution (colored contours) is literally the total number of data points within a distance 0.78 PC-units of each location in PC-space. A similar kernel was used in the production of Figures 2b to Figures 2e.

Several features of the distribution indicate non-Gaussianity. Firstly the mode is displaced away from the mean towards the top left and the separation between contours is greater toward the bottom right than the top left. Secondly the "bulge" that is apparent in the distribution at around $PC1 = -1.5$, $PC2 = -0.5$ associated with a strong southward shifted jet. One quantitative measure of the deviation of the data from Gaussianity is the multivariate skewness of *Mardia and Zemroch* (1975). The multivariate skewness of the ERA-40 data sample is 0.198. A value this large would be unusual given the AR1 model, with a probability of occurring by chance of only 0.0002, estimated from 50000 simulated data-sets. For reference, the estimated probability of a multivariate skewness greater than 0.11 is less than 0.01.

To provide a further test of the robustness of the non-Gaussian features we reproduced the distribution using a six-winter sample of ECMWF 50-member ensemble forecasts from the TIGGE data-set at day fifteen of the forecast. All the features which indicate non-Gaussianity where found to be present in this second distribution and the multivariate skewness of the day 15 TIGGE data was found to be even higher than the ERA-40 data, with a value 0.228.

To investigate the possible explanation for these non-Gaussian features we shall first consider the mean residence time within local regions of PC-space. We define the mean residence time at a point in PC-space to be the mean length of time that trajectories entering a circular region of radius ∼0.78 centered on that point remain within that region. Since the sampling frequency of the data is two days and the data consists of 90 day segments, the shortest observable residence time is two days and the longest 86 days. We exclude trajectories which are within the circle at the start or end of each winter, since the total residence time of such trajectories cannot be known. The radius of the circle was chosen to match the kernel used in calculating the frequency distribution. The two figures are therefore closely related: the frequency distribution giving the total number of data-points within a circular region, and the residence time the average number of consecutive data points in the region.

Figure 2b (color shading) shows the mean residence time calculated for different points in PC-space. The black contours and white contours are as in figure 1c. Only points with frequency (Figure 2a) greater than or equal to 100 are shown. Two things are of note in Figure 2b. Firstly that there is a region of relatively low mean residence time (∼3 days or less) centered on $PC1 = -0.5$, $PC2 = 1$ coincident with the region where the jet has lowest energy. Secondly the longest mean residence times (∼4 days) occur in regions associated with higher energy jets. Noticeably the longest residence time occurs at approximately $PC1 < -2$, $PC2 = 0$ coincident with the noticeable bulge in the frequency distribution seen in Figure 2a. This second feature implies that the existence of bulge in the frequency distribution is a reflection of the long residence times of southward shifted jets.

In tests using 1000 simulated data-sets created by the AR1 model the largest mean residence time obtained was considerably less than that found for the ERA-40 data, being only 3.05 days. More importantly, the largest residence times were found to always lie in a patch near the center of PC-space, 95% of the simulated data-sets being within 0.63 PC-units of the center. This second point, makes the existence of the high residence times of the southward shifted jet and low residence times near the center of the distribution unusual without a non-homogeneous statistical model; i.e. one with parameters that vary with location in PC-space either because of low frequency variations in external boundary conditions (non-stationarity) or simply due to the structure of the dynamical equations themselves.

To examine what such a model might look like, we shall consider the local mean PC-space increments. These are referred to as mean phase-space tendencies by *Franzke et al.* (2007) and are viewed as an estimator of the drift velocity in the context of the Fokker-Planck equation by *Sura et al.* (2005). Essentially they are the expected increment at given location in PC-space. We define the mean PC-space increment at a point as the average vector change in location in PC-space over two days of all data points within 0.78 PC-units of that point. The radius of the circle used is the same as for Figure 2a. The mean PC-space increments are shown in Figure 2c. The streamlines indicate the direction of the mean PC-space increments and the colored shading shows the colors their magnitude.

Several things are noticeable in Figure 2c. Firstly, that the direction of mean flow is inwardly spiraling with the rotational direction indicating that trajectories move in the clockwise direction more frequently than anti-clockwise; i.e. the jet migrates northwards on average. Secondly, the magnitude of the mean PC-space increments is largest at the extremities of the distribution and decreases to zero towards the center. The fact that the mean PC-space increments point inwards and are strongest at the extremities is not surprising. From a statistical point of view it is requirement for the distribution to be approximately stationary. From a physical point of view it is a requirement for the energy and amplitude of the jet to remain bounded. Both these properties would be anticipated from the AR1 model, however the local mean PC-space increments are distorted: for example the inward flow is relatively strong for split jets, but relatively weak for southward shifted jets.

A second means of examining the way in which trajectories move around PC-space is to quantify how rapidly they move. We shall do this by considering the root-mean-squared PC-space increment in different regions of PC-space. These are shown by the colors in Figure 2d. Whereas the colors in Figure 2c show the magnitude of the mean, those in Figure 2d show the mean magnitude. The most striking thing about Figure 2d is the inverse relationship it has with residence time (Figure 2b). Regions which have larger root-mean-squared increments, and by implication evolve more rapidly, have shorter residence time. Quantitative tests indicate that the local mean PC-space increments and root-mean-squared increments are sufficient to explain the observed four day residence times seen in Figure 2b.

4 Flow dependent predictability of the jet

We have so far provided evidence that the behavior of trajectories in PC-space varies with the location. In this section the implications of these results for predictability will be considered. In particular it will be determined if there is evidence that predictability varies with location in PC-space, and whether this variation is consistent with the results of the previous section. To assess the predictability we shall make use of ECMWF ensemble forecast data projected into PC-space. This data is taken from the TIGGE archive (*Park et al.*, 2008), and consists of daily 15 day, 50 member ensemble forecasts spanning six winters from December 2006 to January 2012. Firstly however we shall say briefly what we mean by predictability and how its variation with location in PC-space shall be determined.

The ensemble variance acts as an estimator of forecast uncertainty, larger variance indicating larger uncertainty. The rate at which variance grows can be used as a measure of predictability. Essentially when the growth rate of variance is large, the estimated forecast uncertainty increases rapidly with lead time, and the predictability is lower. Conversely when the variance growth rate is low the estimated forecast uncertainty increases slowly with lead time, and the predictability is higher. It is worth noting here that predictability does not quantify forecast skill; it does however provide an a-priori estimator of the rate at which forecast skill is lost under the assumption that the forecast model is consistent with the physics of the atmosphere and the ensemble is a well constructed sample of the initial uncertainty.

The main questions we wish to answer are, does the predictability of the jet vary systematically with location in PC-space, and can this variation be related to the climatological behavior? To answer these question we shall use the rate of change of ensemble variance as a measure of predictability, and the ensemble mean as a measure of location. We shall use the terms ensemble-mean and ensemble-variance to refer specifically to values calculated within the two-dimensional PC-space.

Figure 2e shows the mean rate of change of ensemble variance (per day) at forecast day six at different locations in PC-space. For each location in PC-space, the mean rate of change of ensemble variance is calculated by averaging the change in ensemble variance in one day over of all forecasts with ensemble mean lying within a circle of radius ~ 0.78 that point. We have chosen to show results from forecast day six since this represents a lead time when the early quasi-exponential phase (*Lorenz*, 2006) of the growth should have largely ended, but the variance is still sufficiently small for the ensemble to be still contained within a local region. In practice however the results and their interpretation are not particularly sensitive to the chosen forecast day.

Two points can be taken from Figure 2e. Firstly, the mean rate of change of ensemble variance depends on the location of the ensemble mean, implying that the trajectories of ensemble members diverge at different rates in different regions of PC-space. Secondly the region of PC-space associated with the largest rate of change of ensemble variance corresponds to the region associated with weak or split jets (Figure 1c) and of largest root-mean-squared increments (Figure 2d).

The dotted line on Figure 2e encloses a region containing rates of change of ensemble variance larger than 80% of the range. We shall call this region the high spread region. Figure 2f shows the mean ensemble variance as a function of forecast day for two mutually exclusive sub-samples of the forecast data. The solid line shows the mean ensemble variance of all forecasts with ensemble mean not entering the high spread region until after day six. The dashed line shows the mean ensemble variance of all forecast with ensemble mean entering the high spread region on forecast day six and not before. Forecasts with ensemble mean entering the high spread region before to forecast day six are neglected. Notably, there is no discernible difference between the mean ensemble variance of the two subsets of forecasts prior to forecast day six. After forecast day six, forecasts with ensemble mean first entering the high spread region on day six have larger mean ensemble variance than those with ensemble mean not entering the high spread region by forecast day six.

The fact that differences between the mean ensemble variances of the two sub-samples of the forecast data only become apparent after entry into the high spread region supports the interpretation of it as a local source of ensemble variance leading to increased forecast uncertainty and lower predictability. An analogy for this would be the region between the "wings" of the Lorenz attractor (*Lorenz*, 1963) associated with rapid separation of trajectories.

5 Summary

In this paper we have examined the evolutionary behavior and predictability of the North-Atlantic eddy driven jet. This was done within a two dimensional principal component space. The main results were as follows. The structure of the frequency distribution within the PC-space is distorted. The distortions are associated with differences in the persistence and rate with which trajectories move through different regions of PC-space. Of particular interest is the region of PC-space associated with weak or split jets. This region has anomalously low persistence and trajectories move rapidly through it. The predictability of the jet is found to be lowest in this region, with the instantaneous growth rate of ensemble variance being anomalously large.

The collocation of this region of low predictability with the region of lowest expected jet speed and kinetic energy, suggests that the predictability depends on the strength of the jet. Weak eddy-driven jets being more susceptible to forcing from the eddy components of the flow than strong eddy-driven jets. The relatively large root-mean-squared PC-space increments in Figure 2d support this idea. The strength and direction of the mean PC-space increments (Figure 2c) imply that when the jet is in the north it is more likely to enter the region associated with weak jets and rapid growth of ensemble variance. This is consistent with the results of *Franzke et al.* (2012) and *Hannachi et al.* (2012) who suggest that when the jet is shifted to the north it will tend to make a transition to a southward shifted jet via wave-breaking. This provides an explanation for the observation of *Frame et al.* (2011) that probabilistic forecast skill is lower when the initial conditions have the jet shifted to the north.

This work was supported via the National Centre for Atmospheric Science – Weather directorate, a collaborative centre of the Natural Environment Research Council. The authors gratefully acknowledge the help of the European Centre for Medium Range Weather Forecasting for providing access to the TIGGE data-set.

References

Christiansen, B. (2009) Is the atmosphere interesting? A projection pursuit study of the circulation in the northern hemisphere winter. *J. Climate, 22*, 1239-1254, doi:10.1175/2008JCLI2633.1.

Frame, T. H. A, M. H. P. Ambaum, S. L. Gray and J. Methven (2011), Ensemble prediction of transitions of the North Atlantic eddy-driven jet, *Q.J.R. Meteorol. Soc., 137*, 1288-1297, doi:10.1002/qj.829.

Franzke, C., A. J. Majda, G. Branstator (2007), The origin of nonlinear signatures of planetary wave dynamics: mean phase space tendencies and contributions from non-Gaussianity. *J. Atmos. Sci., 64*, 3987-4003, doi:10.1175/2006JAS2221.1.

Franzke, C., T. Woollings, O. Martius (2012), Persistent circulation regimes and preferred regime transitions in the North Atlantic. *J. Atmos. Sci., 68*, 2809-2825, doi:10.1175/JAS-D-11-046.1.

Hannachi, A., T. Woollings, K. Fraedrich (2012), The North Atlantic jet stream: a look at preferred positions, paths and transitions. *Q. J. R. Meteorol. Soc., 138*, 862-877, doi:10.1002/qj.959.

Jolliffe, I. T., *Principal component analysis, Second edition*, Springer-Verlag, New York.

Lorenz, E. N. (2006), *Predictability a problem partly solved, in Predictability of weather and climate*, edited by T. Palmer and R. Hagedorn, pp. 40-58, Cambridge University Press

Lorenz, E. N. (1963), Determinisitc nonperiodic flow. *J. Atmos. Sci., 20*, 130-141

Mardia, K. V., P. J. Zemroch (1975), Algorithm AS 84: Measures of multivariate skewness and kurtosis. *Journal of the Royal Statistical Society. Series C (Applied Statistics) 24*, 262-265

Monahan, A. H., J. C. Fyfe (2006), On the nature of zonal jet EOFs. *J. Climate, 19*, 6409-6424.

Monahan, A. H., J. C. Fyfe (2009), How generic are dipolar jet EOFs. *J. Climate, 19*, 6409-6424.

Neumaier A. and T. Schneider (2001), Estimation of parameters and eigenmodes of multivariate autoregressive models.*ACM Trans. Math. Softw., 27*, 27-57.

Park Y. Y., R. Buizza, M. Leutbecher (2008),TIGGE: Preliminary results on comparing and combining ensembles. *Q. J. R. Meteorol. Soc. 134*, 20292050, doi: 10.1002/qj.334.

Schneider T. and A. Neumaier (2001), Algorithm 808: ARfit - A Matlab package for the estimation of parameters and eigenmodes of multivariate autoregressive models. *ACM Trans. Math. Softw., 27*, 58-65.

Stephenson, D. B., V. Pavan, R. Bojariu (2000) Is the North Atlantic oscillation a random walk? *International Journal of Climatology 20*, 118.

Sura, P., M. Newman, C. Penland, P. Sardeshmukh (2005), Multiplicative noise and non-Gaussianity: A paradigm for atmospheric regimes? *J. Atmos. Sci., 62*, 1391-1409

Uppala, S. M., P. W. Kållberg, A. J. Simmons, U. Andrae, V. D. C. Bechtold, M. Fiorino, J. K. Gibson, J. Haseler, A. Hernandez, G. A. Kelly, X. Li, K. Onogi, S. Saarinen, N. Sokka, R. P. Allan, E. Andersson, K. Arpe, M. A. Balmaseda, A. C. M. Beljaars, L. V. D. Berg, J. Bidlot, N. Bormann, S. Caires, F. Chevallier, A. Dethof, M. Dragosavac, M. Fisher, M. Fuentes, S. Hagemann, E. Hólm, B. J. Hoskins, L. Isaksen, P. A. E. M. Janssen, R. Jenne, A. P. Mcnally, J.-F. Mahfouf, J.-J. Morcrette, N. A. Rayner, R. W. Saunders, P. Simon, A. Sterl, K. E. Trenberth, A. Untch, D. Vasiljevic, P. Viterbo, J. Woollen (2005), The ERA-40 re-analysis. *Q. J. R. Meteorol. Soc. 131*, 2961-3012, doi:10.1256/qj.04.176.

Woollings, T., A. Hannachi and B. Hoskins (2011), Variability of the north atlantic eddy-driven jet stream, *Q.J.R. Meteorol. Soc., 136*, 856-868, doi:10.1002/qj.625.

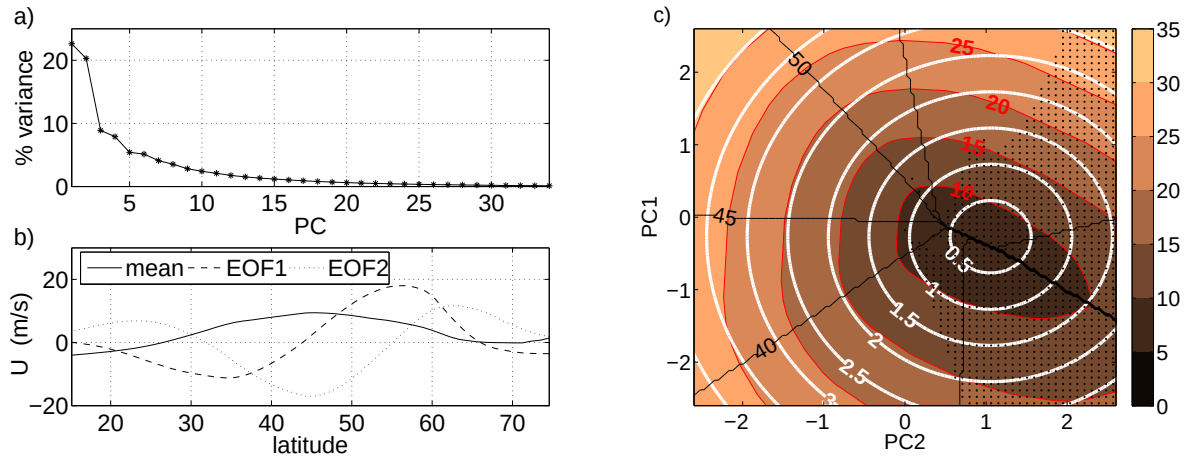

Figure 1: a) Principal component spectrum. b) Mean jet profile and leading two EOFs. c) Summary of the physical properties of the two dimensional PC space. Colored shading/red contours show the wind speed ms^{-1} of the jet maximum. Black radial contours show the latitudinal location (degrees) of the jet maximum. White contours show the square-root of the kinetic energy (normalized by variance) contained in the leading two PCs; this includes the contribution from the mean. Stippling indicates the region of PC space for which two maxima in westerly wind-speed are found.

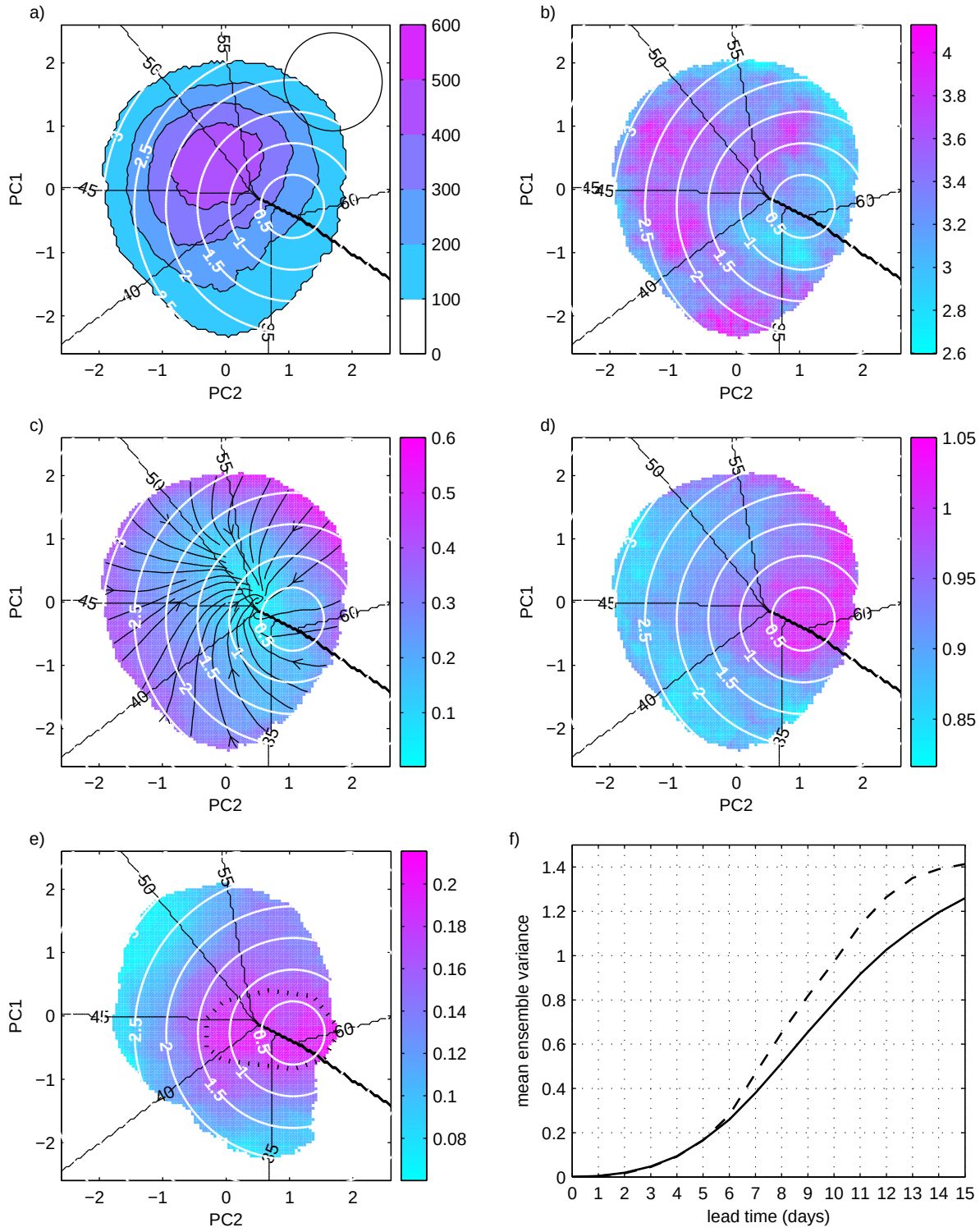

Figure 2: White and black contours as in Figure 1c for all panels. All figures derived from ERA-40 data. (a) Kernel smoothed frequency estimate. Flat circular kernel (shown by black circle) is used. Colors correspond to number of data points within circle. (b) Colors show mean residence time. (c) Streamlines show direction of mean two-day PC-space increments. Colors show corresponding magnitude. (d) Colors show root-mean-squared two day PC-space increments. (e) Colors show the mean rate change of ensemble variance (per day) at forecast day six as a function of the ensemble mean. Estimated from six winters of ECMWF ensemble forecast data. Dashed line encloses the high spread region, containing mean rates of change of ensemble variance grater than 80% of the range. (f) Mean ensemble variance versus forecast day averaged over multiple forecasts. Solid line: averaged over all forecast with ensemble mean not entering high spread region by forecast day six. Dashed line: averaged over all forecast with ensemble mean first entering high spread region on forecast day six.